Published in final edited form as:
Virus Res. 2013 December 26; 178(2): . doi:10.1016/j.virusres.2013.09.008.

Structural and Inhibitor Studies of Norovirus 3C-like Proteases

Daisuke Takahashi[2], **Yunjeong Kim**[1], **Scott Lovell**[3], **Om Prakash**[2], **William C Groutas**[4], and **Kyeong-Ok Chang**[1,*]

[1]Department of Diagnostic Medicine and Pathobiology, College of Veterinary Medicine, Kansas State University, Manhattan, KS 66506

[2]Department of Biochemistry, Kansas State University, 141 Chalmers Hall, Manhattan, KS 66506, USA

[3]Protein Structure Laboratory, Del Shankel Structural Biology Center, University of Kansas, Lawrence, KS 66047

[4]Department of Chemistry, Wichita State University, Wichita, Kansas 67260

Abstract

Noroviruses have a single-stranded, positive sense 7–8 kb RNA genome, which encodes a polyprotein precursor processed by a virus-encoded 3C-like cysteine protease (3CLpro) to generate mature non-structural proteins. Because processing of the polyprotein is essential for virus replication, norovirus 3CLpro has been targeted for the discovery of anti-norovirus small molecule therapeutics. Thus, we performed functional, structural and inhibition studies of norovirus 3CLpro with fluorescence resonance energy transfer (FRET) assay, X-ray crystallography, and NMR spectroscopy with a synthetic protease inhibitor. Three 3CLpro from Norwalk virus (NV, genogroup I), MD145 (genogroup II) and murine norovirus-1 (MNV-1, genogroup V) were optimized for a FRET assay, and compared for the inhibitory activities of a synthetic protease inhibitor (GC376). The apo 3D structures of NV 3CLpro determined with X-ray crystallography and NMR spectroscopy were further analyzed. In addition, the binding mode of NV 3CLpro-GC376 was compared with X-ray crystallography and NMR spectroscopy. The results of this report provide insight into the interaction of NV 3CLpro with substrate/inhibitor for better understanding of the enzyme and antiviral drug development.

1. INTRODUCTION

Noroviruses (genus norovirus in the family *Caliciviridae*) are the most common cause of food- and water-borne acute viral gastroenteritis worldwide (Eckardt and Baumgart, 2011; Green, 2007; Koo et al., 2010; Patel et al., 2009). In the US alone, up to 21 million estimated cases of norovirus-associated gastroenteritis occur each year (2010). Due to its high contagious nature, norovirus outbreaks in cruise ships, army barracks, schools, and hospitals can cause significant morbidity. Furthermore, norovirus infections may lead to fatality in children, the elderly and immuno-compromised patients (Green, 2007). Therefore, norovirus

*To whom correspondence should be addressed: Kyeong-Ok Chang, DVM, MS, PhD: Department of Diagnostic Medicine and Pathobiology, College of Veterinary Medicine, Kansas State University, 1800 Denison Avenue, Manhattan, KS 66506, kchang@vet.ksu.edu; Phone: 785 532-3849; Fax: 785 532-4039.

infection constitutes an important public health problem, as well as a potential bioterrorism threat.

Noroviruses are highly diverse with multiple genotypes (GI to GV) with currently genotype II as the most prevalent in the field. Recently, outbreaks of extremely virulent norovirus, GII.4 Syndey strain (first discovered in Australia in March 2012) continues to spread globally, including the US (Desai et al., 2012; MMWR, 2013; van Beek et al.). This emerging norovirus strain is associated with increased rates of hospitalizations and deaths (Desai et al., 2012). Although norovirus is classified as a Category B bioterrorism agent by CDC, currently there is no norovirus-specific antiviral therapeutics or vaccine partly due to the inability to grow human noroviruses in cell culture (Atmar et al., 2011; Tan and Jiang, 2008). Thus there is an urgent and unmet need for the discovery and development of antiviral therapeutics for the prevention and treatment of norovirus infection. Our group has focused on the discovery and development of small molecules as anti-norovirus therapeutics with enzyme and /or cell based assay systems (Dou et al., 2011a; Dou et al., 2011b; Dou et al., 2012; Dou et al., 2011c; Kim et al., 2011; Mandadapu et al., 2013a; Mandadapu et al., 2012; Mandadapu et al., 2013b; Pokhrel et al., 2012; Tiew et al., 2011).

Noroviruses have a single-stranded, positive sense 7–8 kb RNA genome, which encodes a polyprotein precursor processed by a virus-encoded 3C-like cysteine protease (3CLpro) to generate intermediate or mature functional non-structural proteins. Since processing of the polyprotein is essential for virus replication, viral 3CLpro has been targeted for the discovery of anti-norovirus small molecule therapeutics. Norovirus 3CLpro is characterized with a chymotrypsin-like fold and a cysteine residue acting as a nucleophile in the active site. Norovirus 3CLpro has N-terminal anti-parallel β-sheet domain and C-terminal β-barrel domain and the catalytic site consisting of C139, H30, and E54 is present in the cleft between the domains. The structures of Norwalk virus protease (NV 3CLpro) (Zeitler et al., 2006), Chiba virus protease (CV 3CLpro) (Nakamura et al., 2005), Southampton virus protease (SV 3CLpro) bound with a Michael acceptor peptidyl inhibitor (Hussey et al., 2011), and MNV 3CLpro (Leen et al., 2012) have been determined by X-ray crystallography.

Our group has previously reported the backbone and side-chain resonance assignments of NV 3CLpro by solution NMR spectroscopy (PDB: 2LNC) (Takahashi et al., 2013; Takahashi et al., 2012), and 3D structure of NV 3CLpro without or with a protease inhibitor (GC376) by X-ray crystallography (PDB: 3UR6, 3UR9) (Kim et al., 2012). In addition, the design, synthesis, and evaluation of transition state inhibitors of norovirus 3CLpro, including GC376 (a dipeptidyl compound), was recently reported by our group (Kim et al., 2012; Mandadapu et al., 2012; Tiew et al., 2011). In this study, the proteolytic activities of three 3CLpro from Norwalk virus (NV, genogroup I), MD145 (genogroup II) and murine norovirus-1 (MNV-1, genogroup V) were optimized for a fluorescence resonance energy transfer (FRET) assay, and compared for the inhibitory activities of a synthetic protease inhibitor (GC376). The comparative analysis of 3CLpro from different genogroups of noroviruses may provide further basic knowledge of substrate (inhibitor)-protease interactions, as well as finding broadly active inhibitors against diverse noroviruses. In addition, we describe the comparative analysis of the apo NV 3CLpro and NV 3CLpro-GC376 determined by X-ray crystallography and NMR spectroscopy.

2. MATERIALS AND METHODS

2.1. The expression and purification of proteases from MNV-1

The expression of 3CLpro from NV and MD145 was described previously by our lab (Kim et al., 2012). The 3CLpro from MNV-1 was expressed for the comparative studies in this

study. The multi-alignment of 3CLpro from NV, MD145 and MNV-1 showed that overall amino acid sequences of three 3CLpro are conserved well (Figure 1). The full-length cDNA corresponding to the complete amino acid sequence of MNV-1 3CLpro was amplified using primers of MNV 3CLpro-6hisXba-F (5'-tctagaaaggagatataccATG*catcatcatcatcatcat* gccccagtctccatctggtcc-3', underlined and italic sequences are the start codon and His-tag sequences, respectively) and MNV 3CLpro-Xho-R (5'-ctcgaggcggccgctcatcactggaACTccagagcctcaag-3', underlined sequences are the stop codon). The primers contain cDNA sequences include start and stop codons as well as sequences encoding N-terminal six His-Tag for Ni column purification. The amplicon was cloned into the pET28a vector using enzyme sites of Xba I and Xho I. The plasmid encoding MNV-1 3CLpro was transformed into *E.coli* BL21 cells, and expressed in a regular Luria-Bertani broth media by induction with 1 mM isopropyl β-D-thiogalactopyranoside (IPTG) for 4 hrs at 37 C° in a shaking incubator. The harvested cells were sonicated and ultracentifuged. The expressed protease was soluble and the supernatants were applied to a Ni-NTA affinity column (QIAGEN, Valencia, CA) for purification.

2.2. FRET assay of 3CLpro from NV, MD145 or MNV-1

To increase the sensitivity of norovirus FRET enzyme assay, we used new dye and quencher combination of 5-FAM and QXL520 and compared with the pair of Edans and Dabcyl. The FRET substrate, 5-FAM-DFHLQGP-QXL520 which derived from the P5-P2' residues on the NS1–2/3 cleavage site in ORF1 of NV was synthesized by AnaSpec, Inc (Fremont, CA). The designation of substrate residues for P1 and P1' starts at the scissile bond and counts toward the N- or C-terminus, respectively, as suggested by Schechter and Berger (Schechter and Berger, 1967). We reported the optimization of FRET assay for norovirus 3CLpro with a substrate with the Edans/Dabcyl FRET pair, Edans-DFHLQGP-Dabcyl (Chang et al., 2012), which was also used in this study for comparative analysis. For FRET protease assays, the stock solutions (10 mM) of the substrates were prepared in DMSO, and diluted in assay buffer (20 mM HEPES buffer [pH 8.0] containing 120 mM NaCl, 0.4 mM EDTA, 60 % Glycerol, and 6 mM DTT). The 3CLpro was mixed with substrates in assay buffer in 50 μl in a 96-well black plate (Nalgen Nunc International, Rochester, NY). The fluorescence signals were detected using an excitation and emission wavelength of 490 and 520 nm on a fluorescence microplate reader (FLx800, Biotek, Winooski, VT). The relative fluorescence units (RFU) were calculated for each well by subtracting background fluorescence (substrate only) from the total fluorescence in each well.

2.3. FRET protease assay with GC376

The synthesis and activity of a protease inhibitor compound GC376 against NV 3CLpro and in NV replicon-harboring cells were reported elsewhere (Kim et al., 2012). The dipeptidyl compound was designed based on the substrate specificity and showed excellent inhibitory activity in the enzyme (NV 3CLpro) and cell (NV replicon-harboring cells) based assay (Kim et al., 2012). While GC376 was designed as a protease inhibitor against norovirus 3CLpro, it also demonstrated a broad spectrum activity against related 3C or 3CL protease of picoranviruses and coronarviruses (Kim et al., 2012). The stock solution (10 mM) of GC376 was prepared in DMSO and further diluted in assay buffer. The final concentrations of DMSO in the assay did not exceed 1.5% (vol/vol). The 3CLpro from NV, MD145 or MNV-1 were incubated with various concentrations (0.01 to 50 μM) of GC376 in 25 μl of assay buffer for 30 min at 37 °C. Following incubation, 25 μl of assay buffer containing substrate was added, and the mixtures were incubated in a 96-well black plate at 37 °C for 60 min. The fluorescence signals were detected using an excitation and emission wavelength of 490 and 520 nm on a fluorescence microplate reader. The RFU were calculated for each well, and the dose-dependent FRET inhibition curves were fitted with variable slope (four

parameters) using GraphPad Prism software (La Jolla, CA) in order to determine the IC_{50} values of GC376.

2.4. X-ray crystallography of apo NV 3CLpro and the complex of GC376-NV 3CLpro

We recently reported the crystal structure of apo NV 3CLpro and the complex of GC376-NV 3CLpro (Kim et al., 2012) without detailed analysis. In this study, we report further analysis of apo NV 3CLpro with other previously reported NV 3CLpro or CV 3CLpro (Nakamura et al., 2005; Zeitler et al., 2006), and the complex of GC376-NV 3CLpro was also comparatively analyzed with previous report of the complex of CV 3CLpro-Acetyl-EFQLQ-CH=CHCOO- (Hussey et al., 2011). The interactions of NV 3CLpro and GC376 from X-ray crystallography and NMR spectroscopic analysis was also compared.

2.5. NMR spectroscopic analysis of the interaction of NV 3CLpro with GC376

We previously reported the interaction of NV 3CLpro with a nonspecific protease inhibitor, chymostatin, with NMR spectroscopic analysis (Chang et al., 2012). Using similar approach, we investigated the interaction of NV 3CLpro with GC376 which is a specific inhibitor designed to inhibit norovirus 3CLpro from our lab. Briefly, 2D ^{1}H-^{15}N HSQC spectra were recorded on ^{15}N-labeled NV 3CLpro with different concentrations of GC376, and chemical shift perturbation of the ^{1}H and ^{15}N backbone resonances of NV 3CLpro were observed during titration with the inhibitor. We have previously reported the backbone and side-chain assignments NV 3CLpro by solution NMR spectroscopy (Takahashi et al., 2013; Takahashi et al., 2012). NMR experiments were performed at 25 °C on a Varian 500 MHz VNMR system (Varian Inc., now Agilent Technologies, Palo Alto, CA) equipped with a 5 mm cryogenic triple-resonance inverse detection pulse-field gradient NMR probe. All NMR spectra were processed using NMRPipe (Delaglio et al., 1995), and analyzed with Sparky (Goddard TD., 2006) and CARA software (http://www.nmr.ch) (Keller, 2004). A 0.3 mM of ^{15}N-labeled NV 3CLpro solution dissolved in 50 mM potassium phosphate buffer, pH 6.5, with 200 mM KCl, 5 mM DTT, and 3 mM NaN3 was used to perform the inhibitor titration experiments. Stock solution of GC376 (~50 mM) dissolved in d6-DMSO (Cambridge Isotope Laboratories, Andover, MA) was prepared and added directly into the ^{15}N-labeled NV 3CLpro sample. 2D ^{1}H-^{15}N HSQC spectra of NV 3CLpro were recorded for titration points correspond to GC376/NV 3CLpro molar rations of 0, 0.5, 1.0, 3.0, 5.0. Final concentration of DMSO was 3%, and this concentration has been confirmed to have negligible effect on chemical shift changes of NV 3CL pro in our previous study (Chang et al., 2012). All the spectra were acquired with complex points 1024 × 128 and spectral widths of 14 × 38 ppm in the ^{1}H and ^{15}N dimension. Because chemical shift changes caused by addition of GC376 were relatively large for some residues, additional ^{15}N-edited NOESY-HSQC spectrum (mixing time 100 ms) was measured and analyzed to confirm assignments of backbone amide chemical shift for those residues. Chemical shift changes by the presence of GC376 were characterized using a weighted chemical shift difference (⊗™ = $[1/2\{(\Delta\omega_H)^2+(0.2\ \Delta\omega_N)^2\}]^{1/2}$), where $\Delta\omega_{H,N}$ represents chemical shift changes in the proton and nitrogen dimensions on addition of the inhibitor (Grzesiek et al., 1996).

3. RESULTS

3.1. Proteases from NV, MD145 or MNV-1 were inhibited by GC376 with a similar potency

The optimal concentrations of each protease and the substrate (5-FAM-DFHLQGP-QXL520) were determined for the FRET assay. The optimal concentrations of enzyme and the substrate were 0.03 and 1.6 μM for NV and MD145 3CLpro, respectively, and 0.057 and 1.6 μM for MNV 3CLpro, respectively. These combinations of 3CLpro and substrate gave strong signals with minimal backgrounds. A protease inhibitor, GC376, previously designed

and reported from our lab was used to probe the inhibition of 3CLpro from different noroviruses, NV, MD145, and MNV-1. The IC_{50} values of GC376 against 3CLpro from NV, MD145, and MNV-1 were comparable among tested viruses in the FRET assay (Table 1). However, the IC_{50} values of GC376 against each 3CLpro were 3–5.3 fold lower in the FRET assay using 5-FAM-DFHLQGP-QXL520, compared to those with Edans-DFHLQGP-Dabcyl (Table 1).

3.2. Structure of NV 3CLpro determined by X-ray crystallography and NMR spectroscopy

The structure of NV 3CLpro was determined as dimer by X-ray crystallography in our study (refined to 1.50 Å resolution), which is consistent with the previous reports (Nakamura et al., 2005; Zeitler et al., 2006). The N-terminal end including the α-helix region and the regions between aII and bII β-strands including the loops of C-terminal domain were in closed proximity to the dimeric interface (Figure 3A). When our monomer structure was compared to the previously determined NV 3CLpro by other group (Zeitler et al., 2006), they were closely overlaid with minor variations at the substrate recognition areas including M101-R112, K146-V152 and T161-T166 (Figure 3B). Our solution 3D structure of NV 3CLpro (Figure 4) (Kim et al., 2012) showed minor differences in the secondary structures, compared with the crystal structures of NV or CV 3CLpro previously determined by other groups (Nakamura et al., 2005; Zeitler et al., 2006). The solution structure of NV 3CLpro by NMR spectroscopy has one α-helix in N-terminal domain with 12 β-strands, and its overall organization of α-helix and β-strands are similar to the crystal structures of NV 3CLpro (Zeitler et al., 2006), except extra β-strand consisting of residues 72–77 found in the solution structure (Figure 4B and 5).

3.3. Comparative analysis of the NV 3CLpro-GC376 complex with SV 3CLpro with a Michael acceptor peptidyl inhibitor

We also determined the structure of NV 3CLpro-GC376 complex by X-ray crystallography and the interaction between the enzyme and inhibitor was studied in comparison to a previous report of the complex of SV 3CLpro-Acetyl-EFQLQ-CH=CHCOO- (Hussey et al., 2011). In this complex, GC376 was covalently bound to NV 3CLpro, and multiple hydrogen bonds between the inhibitor and amino acids of the enzyme were identified (Kim et al., 2012). The amino acids including H30, Q 110, T134, C139, H157, A158, A160 were found to participate in the interaction with GC376 (Figure 5A) and Acetyl-EFQLQ-CH=CHCOO- (Figure 5B). Additional amino acids, Arg108 and Lys162 were shown to interact with Acetyl-EFQLQ-CH=CHCOO- (Hussey et al., 2011).

3.4. Chemical shift mapping to study the interaction of NV 3CLpro with GC376

A series of 2D ^{1}H-^{15}N HSQC spectra of NV 3CLpro with increasing concentrations of GC376 were analyzed to identify the residues of NV 3CLpro involved in the interaction with GC376. NMR chemical shift perturbations of backbone amide (^{1}H and ^{15}N) resonances in the ^{1}H-^{15}N HSQC spectra are sensitive probes for changes in chemical environments surrounding amino acid residues and/or in the relative populations of different conformations in protein structural ensemble (Shuker et al., 1996). The weighted chemical shift differences of ^{1}H-^{15}N resonances for NV 3CLpro in the presence of varying concentrations of GC376 were compared to those observed in the absence of the compound (Figure 6A). Significant chemical shift changes were observed in the high concentrations of GC376 (Figures 6A), indicating the specific interaction between NV 3CLpro and GC376. In the presence of 5-fold molar excess of GC376, the residues of NV 3CLpro that showed significantly shifts ($\Delta d \geq 0.07$) were G15, W16, H30*, V31, V32*, H50*, A52, E54*, F55*, Q57*, E74*, K88, R89, G102, A103*, I104, A105, Q110*, L113, V114, H115, G119, G133, T134, G137*, D138, C139, P142, Y143*, V152, H157, T161, K162* and S163* (amino acids for the triad are underlined). The residues that could not be traced out due to the peak

disappearance and/or line broadening are marked with asterisks and the largest positive values ($\Delta d \geq 0.35$) in Figure 6B. The line-broadening effects are likely indicative of chemical exchange on the slow time scale (μs-ms) due to the conformational dynamics of NV 3CLpro interacting with GC376. Figure 6C shows the residues that significantly shifted in the presence GC376 in NV 3CLpro, and the shifted residues include amino acids involved in the hydrogen bonds with the compounds except A158 and A160 (Figure 5A), and other amino acids mostly located in the active sites.

4. DISCUSSION

Norovirus 3CLpro is a cysteine protease with chymotrypsin-like folds with two domains, N-terminal twisted anti-parallel β-sheet domain and C-terminal β-barrel domain. The active site with catalytic residues, C139, H30, and E54 are present in the cleft between the domains. The 3D crystal structures of NV 3CLpro (PDB: 3UR6, 3UR9, 2FYQ, 2FYR) (Kim et al., 2012; Zeitler et al., 2006), CV 3CLpro (PDB: 1WQS) (Nakamura et al., 2005), and Southampton virus (SV) 3CLpro bound with a Michael acceptor peptidyl inhibitor (PDB: 2IPH) (Hussey et al., 2011) have been previously reported. Our multi-alignment of 3CLpro from NV (GI), Southampton (GI), Chiba (GI), MD145 (GII) and MNV-1 (GV) demonstrated that while overall amino acid sequences of all 3CLpro are conserved well, 3CLpro of MNV-1 is more divergent from the other proteases (Figure 1) with especially high divergence in the loop between cI and dI β-strands and C-terminal region of MNV-1 3CLpro. Other than those two regions, however, there is a high homology of 3CLpro including the long loop between cII and dII β-strands (amino acid residues from 119 to 139), which is known to be the major area for the interaction between the enzyme and substrate. The H30, E54 and C139 in the active site are conserved among the proteases except amino acid E54 was replaced with D54 in the MNV 3CLpro (Figure 1). The substrate specificity of noroviruses of different genogroups is also well conserved, and the FRET assays with NV, MD145 and MNV-1 3CLpro showed that they are capable of processing the substrate derived from NS2/3 cleavage sites of NV (Figure 2). The amino acid identities of different norovirus 3CLpro were found to be approximately 90% within the genogroup and 50–70% among different genogroups (Figure 1). The FRET assay also revealed that the 3CLpro from different genogroups were similarly inhibited by a dipeptidyl protease inhibitor, GC376, suggesting that a drug may be developed that are broadly active against multiple norovirus genogroups.

We also examined and compared the structure of NV 3CLpro expressed in our lab with X-ray crystallography and NMR spectroscopy. The crystal structures of apo NV 3CLpro (PDB: 3UR6) and the complex of NV 3CLpro-GC376 (PDB: 3UR9) were recently reported by our group (Kim et al., 2012). NV 3CLpro expressed in our lab exists as dimers by X-ray crystallography, which is consistent with other reports (Nakamura et al., 2005; Zeitler et al., 2006). However, the interface between two molecules (monomers) was different from the previous reported NV 3CLpro (PDB:2FYQ) (Zeitler et al., 2006). It was reported that the regions of bII and cII β-strands of NV 3CLpro were in close proximity to the dimeric interface (Zeitler et al., 2006). However, in our study, the N-terminal end including the α-helix region and the region between aII and bII β-strands including the loop of C-terminal domain were in closed proximity to the dimeric interface (Figure 3A). Interestingly, size exclusion and analytical ultracentrifuge analysis showed that NV 3CLpro exists as a monomer in solution (Chang et al., 2012; Takahashi et al., 2013). These findings suggest that monomer/dimer state of NV 3CLpro may depend on the experimental conditions.

Overlay of our apo NV 3CLpro with NV 3CLpro available in the protein database (PDB: 2FYQ) (Zeitler et al., 2006) showed that their overall fold was well conserved with minor differences in the regions of M101-R112, K146-V152 and T161-T166 (Figure 3). The NMR

structure of NV 3CLpro in our study also showed minor differences in those regions with overall conserved folds. It was demonstrated that the C-terminal domain of NV 3CLpro is predominantly involved in the interaction with the substrate, in which the binding occurs in the manner of anti-parallel β-sheet via hydrogen bond network between the substrate and the protease. Thus, the observed differences are speculated to be originated from high internal dynamics in those regions that are involved in the interaction of substrates. The regions with minor differences in structure encompass the highly disordered loop (L121-G140), most of which have no visible electron densities in the norovirus 3CLpro crystal structure (T123-G133) (Nakamura et al., 2005; Zeitler et al., 2006). The amino acids in the disordered loop are highly conserved among norovirus proteases, suggesting their crucial role in the interactions with substrates. Our apo NV 3CLpro also demonstrated that the loop had no visible electron densities (Figure 3).

We have shown that GC376 is effective in inhibiting norovirus 3CLpro and in replication of noroviruses in cell based assays including NV replicon-harboring cells and MNV-1 (Kim et al., 2012; Tiew et al., 2011). We also previously reported the co-crystallization of enzyme-inhibitor by X-ray crystallography (Kim et al., 2012). The structure of NV 3CLpro-GC376 complex showed that the dipeptidyl compound was covalently bound to Cys residue of the enzyme (Figure 5A). Also the structure identified several hydrogen bonds between the inhibitor and amino acid residues including H30, Q110, T134, C139, H157, A158, and A160 in the protease. These amino acids were shown to be also involved in the interaction of SV 3CLpro with Acetyl-EFQLQ-CH=CHCOO- (Figure 5B modified with PDB: 2IPH, Hussey et al., 2011). Of note, additional two amino acids, R108 and K162 in SV 3CLpro, were shown to interact with Acetyl-EFQLQ-CH=CHCOO-, most likely due to its longer length compared to GC376. In this study, we determined the interaction of NV 3CLpro and GC376 with NMR spectroscopy and compared it to that with X-ray crystallography. In NMR structure of the complex, H30, Q110, T134, C139 and H157 among the amino acids showing hydrogen bonds with GC376 were significantly shifted (Figure 6). Furthermore, additional amino acids adjacent to those directly interacting with the inhibitor were significantly affected as shown in Figure 6C. These findings are consistent with those as determined in the crystal structure using X-ray diffraction. It was reported that NV 3CLpro has the catalytic triad in the active site with a C139 (the nucleophile), H30 (the general base), and G54 (an anion that correctly positions the imidazole ring of the active site H) (Zeitler et al., 2006). It was also suggested that some norovirus 3CLpro (such as CV 3CLpro) may have the catalytic dyad (Nakamura et al., 2005). In this study with NV 3CLpro, significant conformational changes were also observed the residues of the catalytic triad in the presence of inhibitor such as GC376 chymostatin (Kim et al., 2012).

We previously reported chymostatin inhibit norovirus 3CLpro in the FRET assay, but it is not effective on inhibiting virus replication in cell based system (Chang et al., 2012). Chymostatin is a tetrapetide protease inhibitor with F at P1 and L (V or I) at P2, capreomycidine at P3, and N-alpha-carbonyl at P4 sites. In that study, the chemical shift mapping by the interaction of NV 3CLpro and chymostatin was also investigated using NMR chemical shift perturbation method. Amino acids residues involved in the interaction between NV 3CLpro with chymostatin include E54, Q110, C139 and H157. Overall profiles of amino acids involved (shifted) in the interaction with chymostatin or GC376 were similar, but more amino acids were shifted by chymostatin (Chang et al., 2012) in compared to those by GC376. The size-differences between chymostatin (tetrapeptidyl) and GC376 (dipeptidyl) may be the reason for why more amino acids were shifted by chymostatin. Nonetheless, GC376 has comparable (or better) activity than chymostatin in inhibiting norovirus 3CLpros in the enzyme assay, which suggests that the dipeptidyl structure has a minimum requirement for the enzyme inhibition. It is also noted that while GC376 is active

in the cell culture systems including the replicon-harboring cells and MNV-2, chymostatin did not show any activity in cell-based assay.

In summary, we performed comparative studies of 3CLpro from three noroviruses of different genogroups and comparative structural analysis of apo NV 3CLpro or NV 3CLpro-GC376 complex with X-ray crystallography and NMR spectroscopy. The results of this report provide insight of the structures NV 3CLpro as well as substrate/inhibitor interaction for better understanding of the enzyme function and antiviral drug development.

Acknowledgments

We are grateful to David George for technical assistance. This work was supported by NIH grant AI081891. Use of the Advanced Photon Source was supported by the U.S. Department of Energy under Contract DE-AC02-06CH11357. Use of the KU COBRE-PSF Protein Structure Laboratory was supported by NIH grant P20 RR-17708. NMR instrumentation at KSU was funded by NIH grant (S10-RR 025441).

REFERENCES

Atmar RL, Bernstein DI, Harro CD, Al-Ibrahim MS, Chen WH, Ferreira J, Estes MK, Graham DY, Opekun AR, Richardson C, Mendelman PM. Norovirus vaccine against experimental human Norwalk Virus illness. N Engl J Med. 2011; 365(23):2178–2187. [PubMed: 22150036]

CDC. 2010. www.cdc.gov/ncidod/dvrd/revb/gastro/norovirus-factsheet.htm

Chang KO, Takahashi D, Prakash O, Kim Y. Characterization and inhibition of norovirus proteases of genogroups I and II using a fluorescence resonance energy transfer assay. Virology. 2012; 423(2): 125–133. [PubMed: 22200497]

Delaglio F, Grzesiek S, Vuister GW, Zhu G, Pfeifer J, Bax A. NMRPipe: a multidimensional spectral processing system based on UNIX pipes. J Biomol NMR. 1995; 6(3):277–293. [PubMed: 8520220]

Desai R, Hembree CD, Handel A, Matthews JE, Dickey BW, McDonald S, Hall AJ, Parashar UD, Leon JS, Lopman B. Severe outcomes are associated with genogroup 2 genotype 4 norovirus outbreaks: a systematic literature review. Clin Infect Dis. 2012; 55(2):189–193. [PubMed: 22491335]

Dou D, He G, Mandadapu SR, Aravapalli S, Kim Y, Chang KO, Groutas WC. Inhibition of noroviruses by piperazine derivatives. Bioorg Med Chem Lett. 2011a; 22(1):377–379. [PubMed: 22119464]

Dou D, Mandadapu SR, Alliston KR, Kim Y, Chang KO, Groutas WC. Design and synthesis of inhibitors of noroviruses by scaffold hopping. Bioorg Med Chem. 2011b; 19(19):5749–5755. [PubMed: 21893416]

Dou D, Mandadapu SR, Alliston KR, Kim Y, Chang KO, Groutas WC. Cyclosulfamide-based derivatives as inhibitors of noroviruses. Eur J Med Chem. 2012; 47(1):59–64. [PubMed: 22063754]

Dou D, Tiew KC, He G, Mandadapu SR, Aravapalli S, Alliston KR, Kim Y, Chang KO, Groutas WC. Potent inhibition of Norwalk virus by cyclic sulfamide derivatives. Bioorg Med Chem. 2011c; 19(20):5975–5983. [PubMed: 21925886]

Eckardt AJ, Baumgart DC. Viral gastroenteritis in adults. Recent Pat Antiinfect Drug Discov. 2011; 6(1):54–63. [PubMed: 21210762]

Goddard, TD.; K, D. SPARKY 3.113. San Francisco: University of California; 2006.

Green, KY. Caliciviruses: The Noroviruses. In: Knipe, DM.; Howley, PM., editors. Fields Virology. 5th ed.. Vol. 1. Philadelphia: Lippincott Williams & Wilkins; 2007. p. 949-980.

Grzesiek S, Bax A, Clore GM, Gronenborn AM, Hu JS, Kaufman J, Palmer I, Stahl SJ, Wingfield PT. The solution structure of HIV-1 Nef reveals an unexpected fold and permits delineation of the binding surface for the SH3 domain of Hck tyrosine protein kinase. Nat Struct Biol. 1996; 3(4): 340–345. [PubMed: 8599760]

Hussey RJ, Coates L, Gill RS, Erskine PT, Coker SF, Mitchell E, Cooper JB, Wood S, Broadbridge R, Clarke IN, Lambden PR, Shoolingin-Jordan PM. A Structural Study of Norovirus 3C Protease Specificity: Binding of a Designed Active Site-Directed Peptide Inhibitor. Biochemistry. 2011; 50:240–249. [PubMed: 21128685]

Keller, R. The computer aided resonance assignment tutorial. Switzerland: Verlag Goldau; 2004.

Kim Y, Lovell S, Tiew KC, Mandadapu SR, Alliston KR, Battaile KP, Groutas WC, Chang KO. Broad-Spectrum Antivirals against 3C or 3C-Like Proteases of Picornaviruses, Noroviruses, and Coronaviruses. J Virol. 2012; 86(21):11754–11762. [PubMed: 22915796]

Kim Y, Thapa M, Hua DH, Chang KO. Biodegradable nanogels for oral delivery of interferon for norovirus infection. Antiviral Res. 2011; 89(2):165–173. [PubMed: 21144866]

Koo HL, Ajami N, Atmar RL, DuPont HL. Noroviruses: The leading cause of gastroenteritis worldwide. Discov Med. 2010; 10(50):61–70. [PubMed: 20670600]

Leen EN, Baeza G, Curry S. Structure of a murine norovirus NS6 protease-product complex revealed by adventitious crystallisation. PLoS One. 2012; 7(6):e38723. [PubMed: 22685603]

Mandadapu SR, Gunnam MR, Tiew KC, Uy RA, Prior AM, Alliston KR, Hua DH, Kim Y, Chang KO, Groutas WC. Inhibition of norovirus 3CL protease by bisulfite adducts of transition state inhibitors. Bioorg Med Chem Lett. 2013a; 23(1):62–65. [PubMed: 23218713]

Mandadapu SR, Weerawarna PM, Gunnam MR, Alliston KR, Kim Y, Chang KO, Groutas WC. Potent Inhibition of Norwalk Virus 3C Protease by Peptidyl α-Ketoamides and α-Ketoheterocycles. Bioorg Med Chem. 2012 In press.

Mandadapu SR, Weerawarna PM, Prior AM, Uy RAZ, Aravapalli S, Alliston KR, Lushington GH, Kim Y, Hua DH, Chang K-O, Groutas WC. Macrocyclic inhibitors of 3C and 3C-like proteases of picornavirus, norovirus, and coronavirus. Bioorganic & Medicinal Chemistry Letters. 2013b; 23:3709–3712. [PubMed: 23727045]

MMWR. Notes from the Field: Emergence of New Norovirus Strain GII.4 Sydney — United States, 2012. In: CDC. , editor. 2013. p. 5562(03) vols.

Nakamura K, Someya Y, Kumasaka T, Ueno G, Yamamoto M, Sato T, Takeda N, Miyamura T, Tanaka N. A norovirus protease structure provides insights into active and substrate binding site integrity. J Virol. 2005; 79(21):13685–13693. [PubMed: 16227288]

Patel MM, Hall AJ, Vinje J, Parashara UD. Noroviruses: A comprehensive review. Journal of Clinical Virology. 2009; 44(1):1–8. [PubMed: 19084472]

Pokhrel L, Kim Y, Nguyen TD, Prior AM, Lu J, Chang KO, Hua DH. Synthesis and anti-norovirus activity of pyranobenzopyrone compounds. Bioorg Med Chem Lett. 2012; 22(10):3480–3484. [PubMed: 22513282]

Schechter I, Berger A. On the size of the active site in proteases. I. Papain. Biochem Biophys Res Commun. 1967; 27(2):157–162. [PubMed: 6035483]

Shuker SB, Hajduk PJ, Meadows RP, Fesik SW. Discovering high-affinity ligands for proteins: SAR by NMR. Science. 1996; 274(5292):1531–1534. [PubMed: 8929414]

Takahashi D, Hiromasa Y, Kim Y, Anbanandam A, Yao X, Chang KO, Prakash O. Structural and dynamics characterization of norovirus protease. Protein Sci. 2013; 22(3):347–357. [PubMed: 23319456]

Takahashi D, Kim Y, Chang KO, Anbanandam A, Prakash O. Backbone and side-chain (1)H, (1)(5)N, and (1)(3)C resonance assignments of Norwalk virus protease. Biomol NMR Assign. 2012; 6(1): 19–21. [PubMed: 21647610]

Tan M, Jiang X. Norovirus gastroenteritis, increased understanding and future antiviral options. Curr Opin Investig Drugs. 2008; 9(2):146–151.

Tiew KC, He G, Aravapalli S, Mandadapu SR, Gunnam MR, Alliston KR, Lushington GH, Kim Y, Chang KO, Groutas WC. Design, synthesis, and evaluation of inhibitors of Norwalk virus 3C protease. Bioorg Med Chem Lett. 2011; 21(18):5315–5319. [PubMed: 21802286]

van Beek J, Ambert-Balay K, Botteldoorn N, Eden JS, Fonager J, Hewitt J, Iritani N, Kroneman A, Vennema H, Vinje J, White PA, Koopmans M. NoroNet. Indications for worldwide increased norovirus activity associated with emergence of a new variant of genotype II.4, late. Euro Surveill. 2012; 18(1):8–9. [PubMed: 23305715]

Zeitler CE, Estes MK, Venkataram Prasad BV. X-ray crystallographic structure of the Norwalk virus protease at 1.5-A resolution. J Virol. 2006; 80(10):5050–5058. [PubMed: 16641296]

Highlights

- Three norovirus 3C-like proteases from different genogroups were optimized for a FRET assay
- The apo 3D structures of Norwalk virus 3C-like protease were further analyzed
- The binding mode of Norwalk virus 3C-like protease with a synthetic inhibitor (GC376) was analyzed

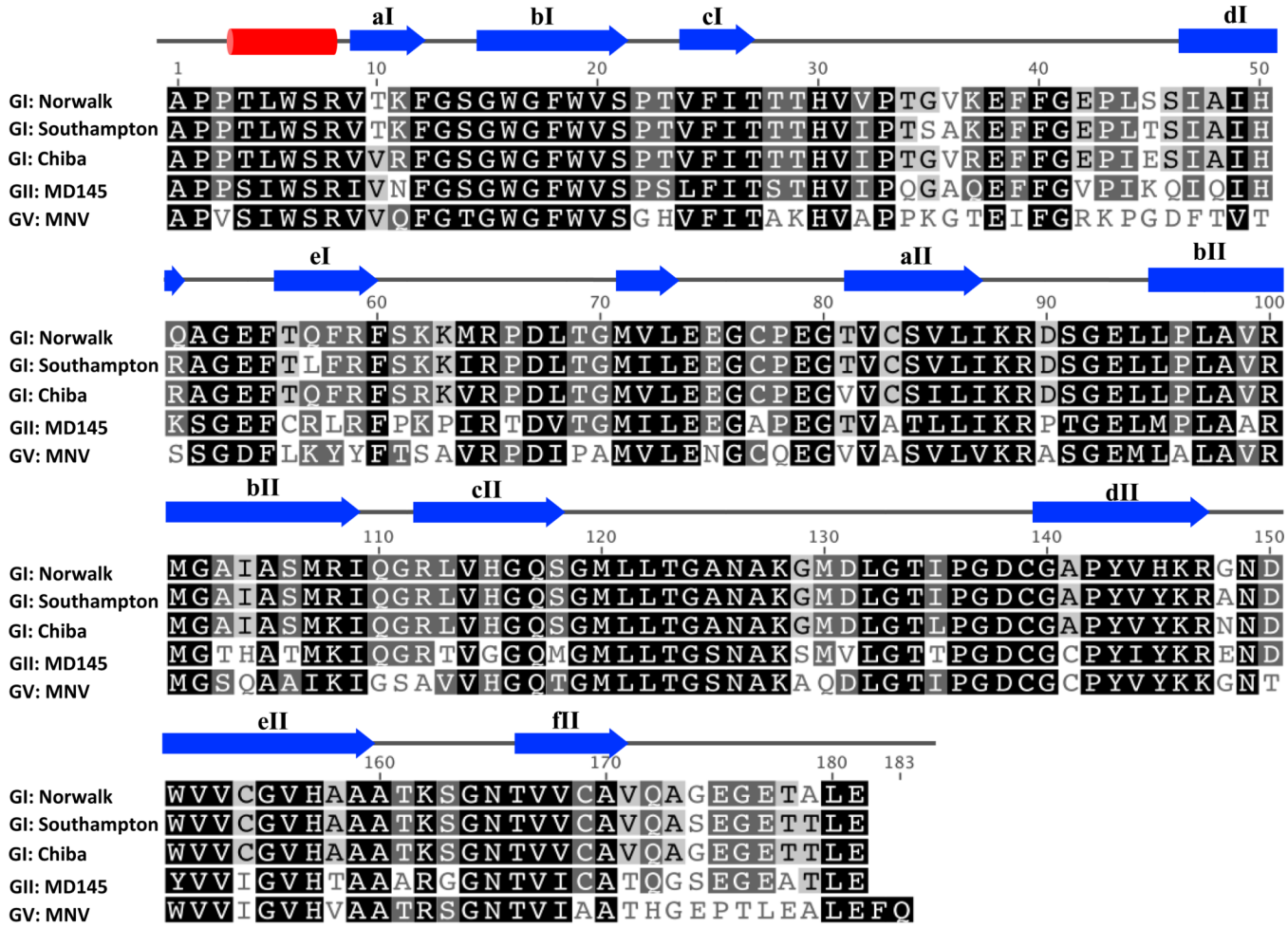

Figure 1.

Multi-alignment of 3CLpro from various GI, GII and GV norovirus strains. A red box and blue arrows are projected as α-helix and β-strands of the proteases determined in this study (by NMR spectroscopy), respectively.

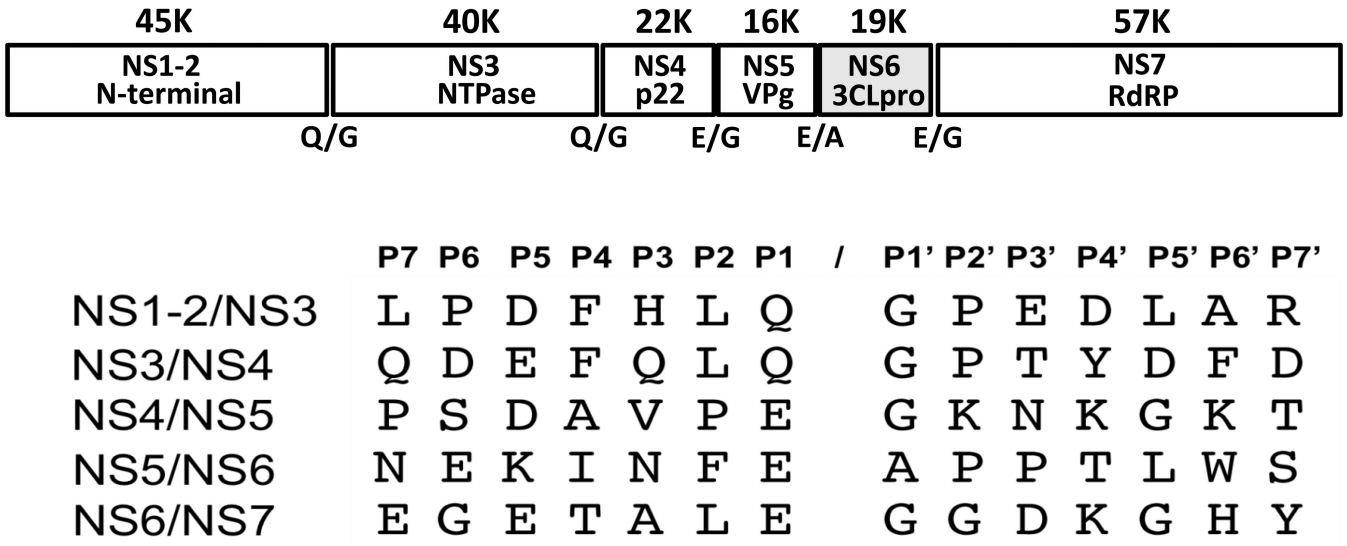

Figure 2.
Genomic organization of Norwalk virus open reading frame (ORF) 1 with 3CLpro recognition sites. NS indicates nonstructural protein. RdRP indicates RNA-dependent RNA polymerase.

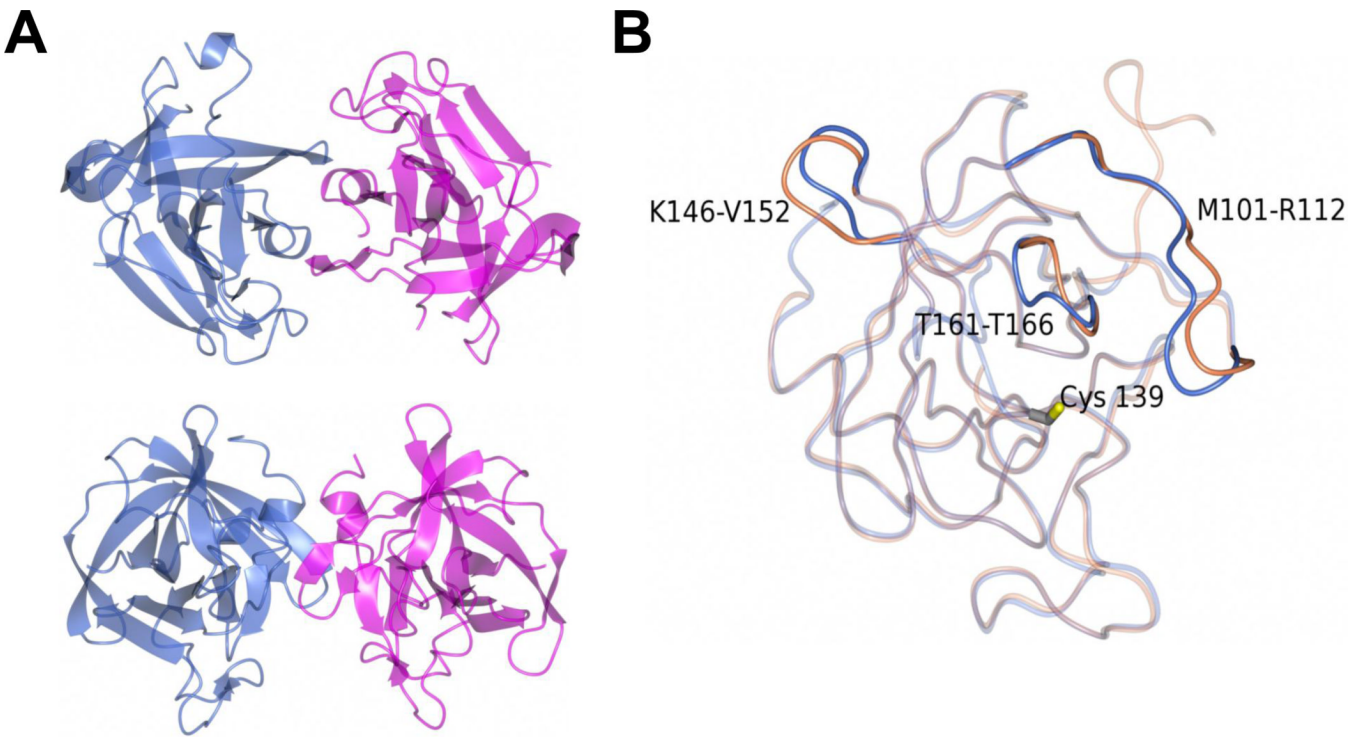

Figure 3.

A. Non-crystallograhic symmetry (NCS) dimer of NV 3CLpro showing chain A (magenta) and chain B (blue). Upper: View along the NCS 2-fold axis. Lower: Viewed normal to the NCS axis. B. Comparison of apo NV 3CLpro (PDB: 3UR6) chain B (blue) with NV 3CL pro from PDB: 2FYQ (tan). The main differences are highlighted and the active site residue Cys 139 is indicated.

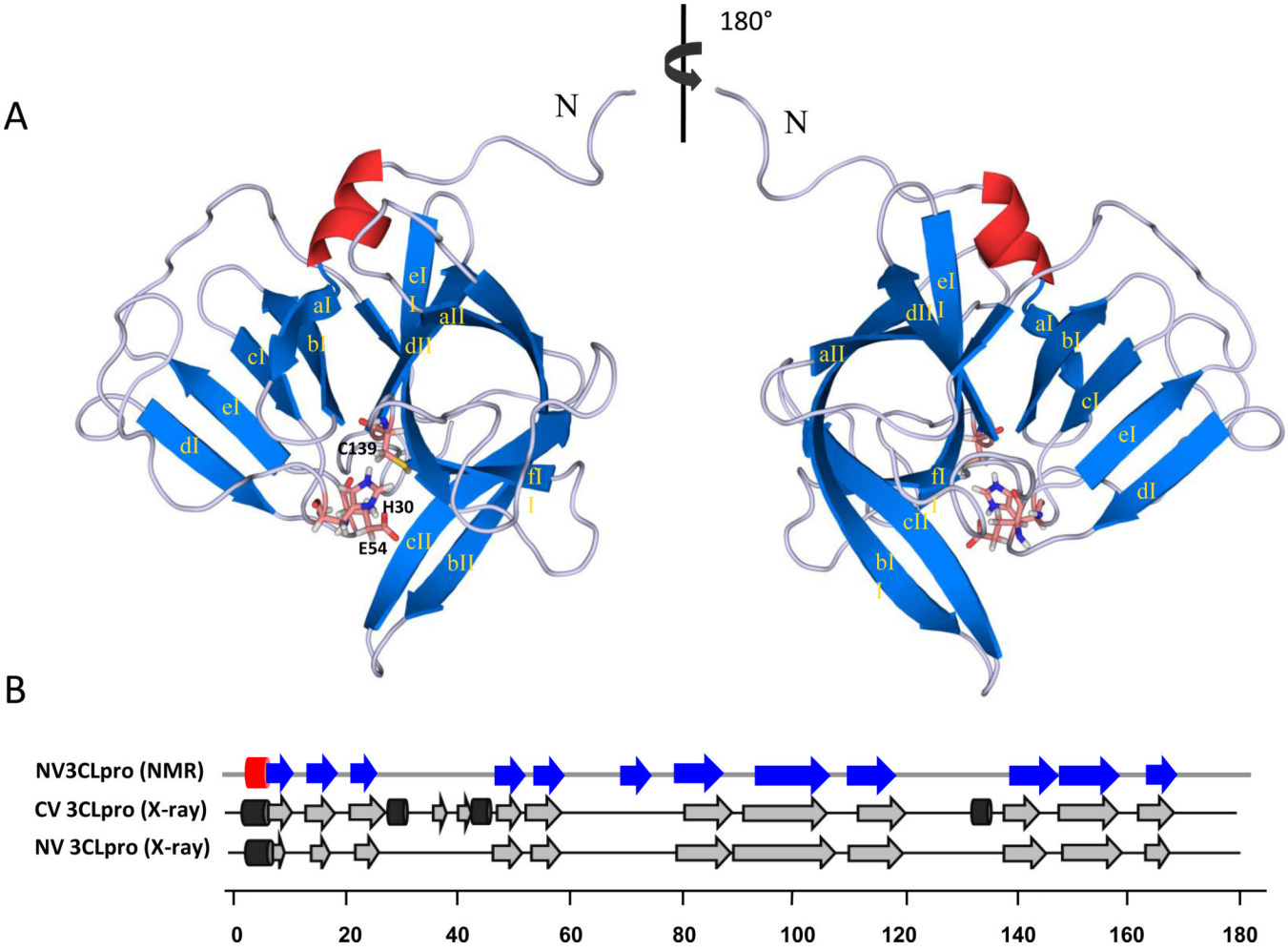

Figure 4.

NV 3CLpro solution structure determined by NMR. A. Ribbon representation of the solution structure of NV 3CLpro with active site residues (H30, E54, and C139) depicted as sticks. β-strands are labeled in the figure. B. The secondary structures of NV 3CLpro in solution compared with those determined by CV 3CLpro and NV 3CLpro by X-ray crystallography (arrows indicate β-barrel, etc. and the box indicates α-helix).

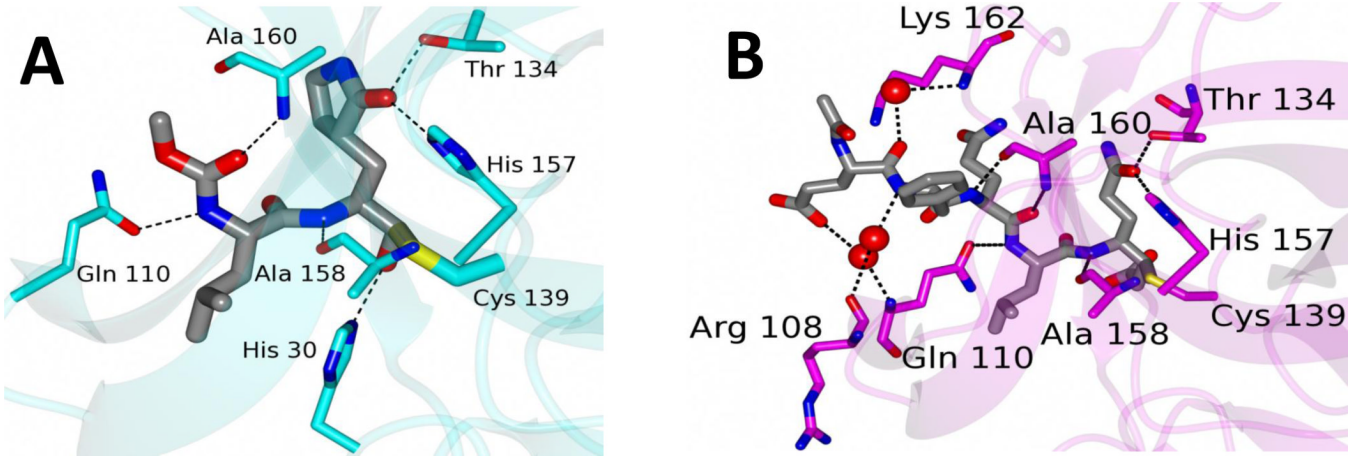

Figure 5.

Interaction of NV 3CLpro and GC376 in comparison to SV 3CLpro with a Michael acceptor peptidyl inhibitor. A. Interaction between NV 3CLpro and a dipeptidyl compound GC376. B. Binding interaction between Southampton norovirus 3CLpro with Acetyl-EFQLQ-CH=CHCOO- (Hussey et al., 2011).

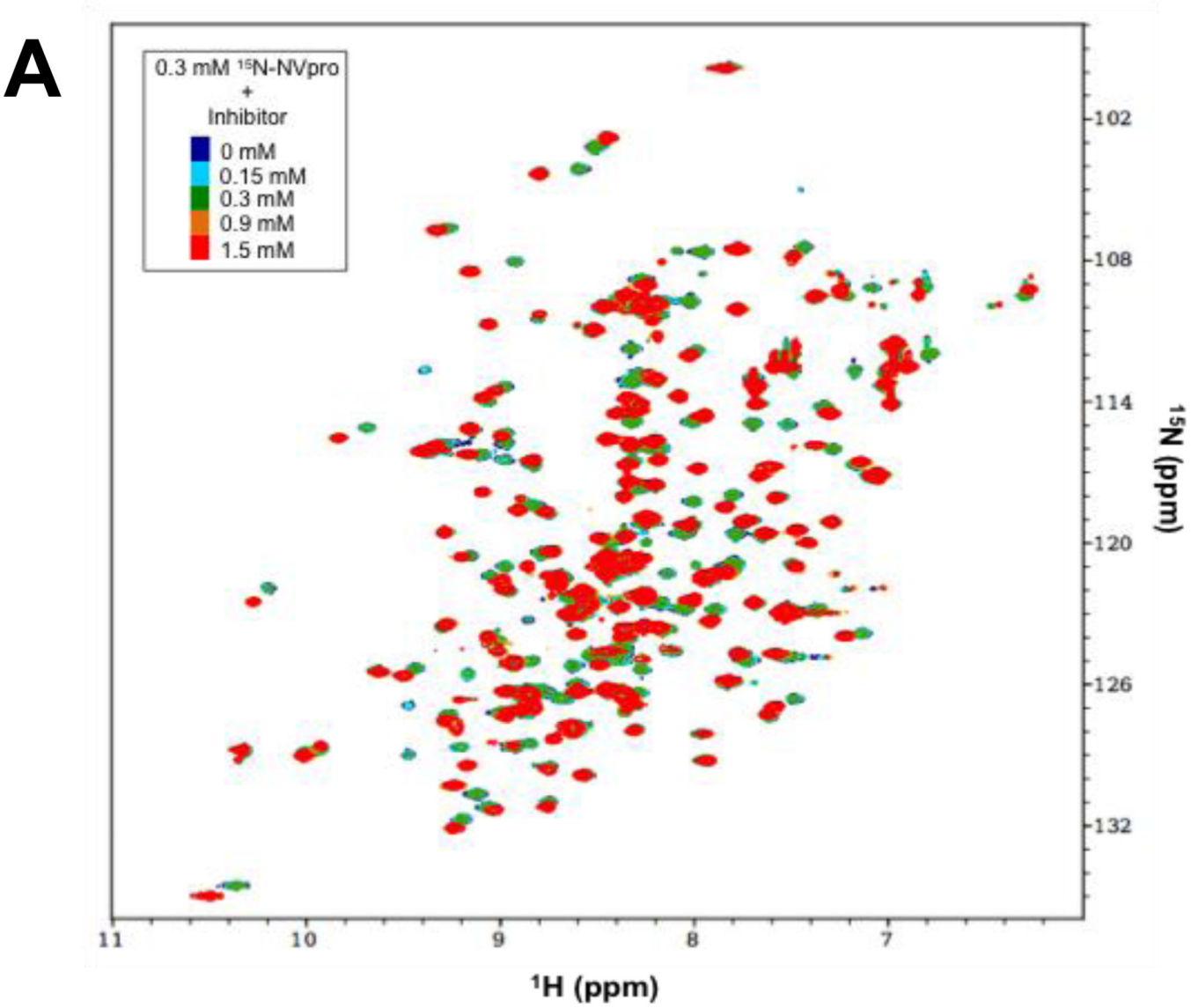

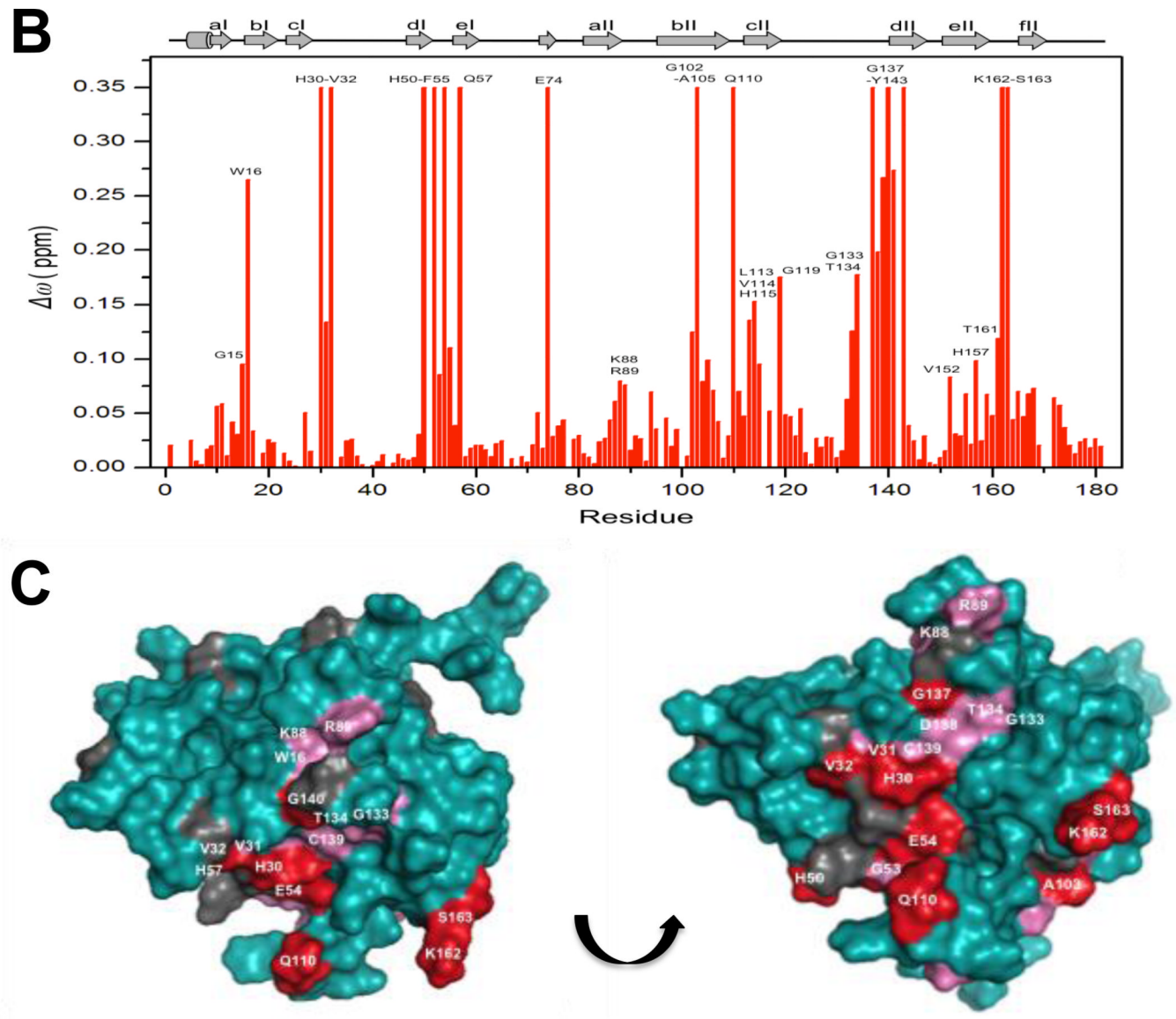

Figure 6.

Effect of a protease inhibitor binding on the structure of NV 3CLpro assessed by chemical shift mapping. A. Overlay of a series of ^{1}H-^{15}N HSQC spectra of NV 3CLpro with increasing concentrations of GC376. B. Plot of chemical shift difference values (Δw) as a function of residue number. Δw values are mapped onto the NV 3CLpro structure. C. Residues that show peak disappearance are indicated by red colors and residues with Δw more than 0.1 ppm by pink color.

Table 1

The effects of GC373 on 3CLpro from NV, MD145 or MNV-1 in the FRET assay

	Inhibition [IC_{50} (μM)] against recombinant 3CLpro*					
	Edans-DFHLQGP-Dabsyl (Kim et al., 2012)#			5-FAM-DFHLQGP-QXL520		
	NV	MD145	MNV-1	NV	MD145	MNV-1
GC376	0.64	1.18	1.4	0.12	0.4	0.38

*The IC_{50} values were averages of two or three independent tests.

#The IC_{50} values of NV and MD145 with this substrate was reported previously (Kim et al., 2012).